



ELSEVIER

Contents lists available at ScienceDirect

## Measurement

journal homepage: [www.elsevier.com/locate/measurement](http://www.elsevier.com/locate/measurement)

## Measurement of human response to tactile temperature sensing using stochastic system identification

T. Eusner<sup>a</sup>, M. Cullinan<sup>a,\*</sup>, C. Ruggiero<sup>a</sup>, N. Zarrouati<sup>a</sup>, A. Chepko<sup>b</sup>

<sup>a</sup> Department of Mechanical Engineering, Massachusetts Institute of Technology, Cambridge, MA 02139, United States

<sup>b</sup> Department of Aeronautics and Astronautics, Massachusetts Institute of Technology, Cambridge, MA 02139, United States

### ARTICLE INFO

#### Article history:

Received 22 January 2010

Accepted 24 February 2011

Available online 1 March 2011

#### Keywords:

Stochastic system identification

Tactile sensing

Vibratory signals

Human transfer function

### ABSTRACT

Tactile response is limited for many operations that are preformed in extreme environments due to bulky equipment or the limitations of the human body. In order to allow a user in extreme environments to regain some of their temperature–tactile response, a glove was developed that converts temperature into a vibration felt by the user. An RTD was attached to the glove and connected to a microcontroller. This microcontroller converted temperature into a voltage and transmitted it to a micromotor that controlled the vibration felt by the user. Through this scheme, the user was able to identify a temperature increase with a 4 s delay. This paper also presents the system response of the glove to a temperature impulse. Using this system transfer function, it is possible to make improvements to the glove to reduce the overall delay between the glove sensing a temperature and the user recognizing the temperature change.

© 2011 Elsevier Ltd. All rights reserved.

### 1. Introduction

Sensory substitution has been a subject of research since the 1960's when Paul Bach-y-Rita looked at the idea of using tactile sensations to relay visual or other sensory information [1]. The concept is based on the brain's plasticity—its ability to adapt or remap connections when one of the senses is absent. A deteriorated sense is often the result of poor or no communication between the sensing organs (ex. eyes) and the brain. However, the section of the brain that interprets the signal is still intact, so if information is relayed through a different sensory system (ex. tactile sensation), the brain can learn to interpret the information in a new way. To date, most sensory substitution systems are focused on providing visual or auditory information via tactile stimulation in blind or deaf patients.

There has been other research conducted on relaying tactile information from one area of the body to another, as in the case of Bach-y-Rita's experiment with restoring

touch perception to leprosy patients. In that research, force information from the fingertips was relayed to an electrode on the forehead and, after training on the device, patients perceived the sensations on their foreheads as if they had originated at their fingertips – the device served to extend their perception of sensation to the site of the force application [2]. Tactile–tactile substitution was also investigated by Bach-y-Rita for astronaut space suit gloves [3]. The motivation for this research stemmed from the difficulty astronauts experience when handling objects in space. Due to the bulkiness of the pressurized gloves, force and fine-pressure sensations are absent. This causes fast fatigue of the hands that tend to over-grip objects in the absence of tactile feedback. In the experiment, force sensors were applied to the outside of the gloves, and sensory information was relayed to electrodes on the astronaut's stomach.

The motivation for this research device stemmed from additional tactile information that is lost when wearing bulky gloves–temperature. For astronauts operating in extreme temperature environments, the temperature sensations of objects they handle are also lost. As astronauts

\* Corresponding author.

E-mail address: [mcullin1@mit.edu](mailto:mcullin1@mit.edu) (M. Cullinan).

return to the moon and spend more time on spacewalks, temperature information of handled objects will become more important. In an environment that already requires a heavy reliance on visual cues, one more instrument dial to read adds to the information overload of the visual channel. The ability to sense temperatures via tactile stimulation will increase environmental awareness without overloading the brain's processing systems. A temperature-to-tactile system can also be useful for medical patients who suffer from loss of sensation in their hands and for workers in extreme terrestrial environments, such as firefighters.

While there do not appear to be any patents or papers that implement the conversion of temperature information to tactile stimulation via a handheld device, a number of related ideas have been proposed. A similar apparatus converts visual or auditory information into a sensation of localized cooling on the skin [4]. Cooling is achieved by covering the skin with an insulating medium and then selectively opening gates in the medium to release pockets of body heat. Another substitution device consists of translating visual information into tactile information via thermal imaging to assist blind patients [5]. Thermal images are taken to represent the environment and are subsequently coded to a tactile pin system. According to the research, representing a real-world visual environment is easier to interpret when using infrared wavelengths as opposed to the visual spectrum. Another similar concept explored remote sensing for applications in tele-operation techniques [6]. A multi-modal sensing finger was developed that could sense the main types of tactile sensation: contact pressure, hardness, texture, temperature, slip, profile, thermal conductivity. This information was then relayed to an integrated glove with actuators to represent the sensed information.

## 2. Apparatus design

### 2.1. Glove system design

The goal of the proposed device is to convert a measured temperature into a vibration that a user can physically sense. A block diagram of how such a system would work is shown in Fig. 1. The user of the glove sensing system presses on the surface of an object in order to determine the object's temperature.

A piezoresistive force sensor is located on the palm of the glove and acts as an on/off switch for the system. When

a user applies enough force to an object's surface, a voltage will inform the microcontroller to turn on the temperature sensor and begin to record temperature.

A temperature sensor is also located on the palm of the glove. Once enough force is applied to the object and the temperature sensor has turned on, the temperature sensor begins to determine the temperature of the given surface. The sensor sends a voltage to the microcontroller, where it is processed and used to determine the voltage input to the micromotor, providing vibration feedback to the user.

After a temperature is determined, it is transferred to the skin of the user of the glove via a vibrating micromotor. The micromotor will vibrate at different frequencies allowing the user to identify the temperature of the surface he/she is touching with reasonable accuracy.

A circuit diagram of the system is shown in Fig. 2, and a photograph of the physical system is shown in Fig. 3. As shown in Fig. 2, the temperature sensor is essentially a variable resistor which is placed in a Wheatstone bridge configuration so that its resistance change can be accurately measured. Voltage is applied to this Wheatstone bridge via a voltage regulator, and the output voltage of the Wheatstone bridge varies as the resistance of the RTD changes. This output voltage is amplified through an instrumentation amplifier, and then sent to the microcontroller to be analyzed. The microcontroller used was a Luminary Micro, Stellaris microcontroller (Model No. LM3S8962) [7]. The force sensor is connected to an inverting amplifier to amplify the voltage output, which is then sent to the microcontroller for analysis. Finally, the microcontroller uses the temperature sensor and force sensor inputs to control the micromotor; the output of the system. The output voltage of the microcontroller is pulse width modulated (PWM) in order to drive the micromotor. The PWM output voltage is amplified by an inverting power amplifier, which is then used to drive the micromotor.

### 2.2. Temperature sensor

An Omega flat profile, thin film Platinum resistance temperature detector (RTD) (Part No. F2020-100-B-100) was used to sense the temperature of a surface in the glove system [8]. A photograph of the RTD used is shown in Fig. 4. The sensor is 2 mm × 2 mm in dimension, allowing it to be placed on a glove without interfering with the user's ability to grasp objects or perform necessary tasks. The useful range of the sensor is -50–500 °C, which is a

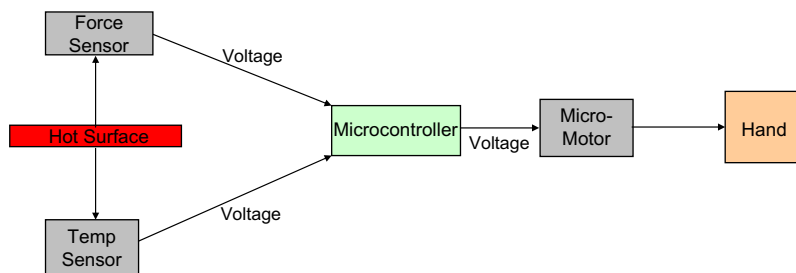


Fig. 1. Block diagram of the proposed glove system.

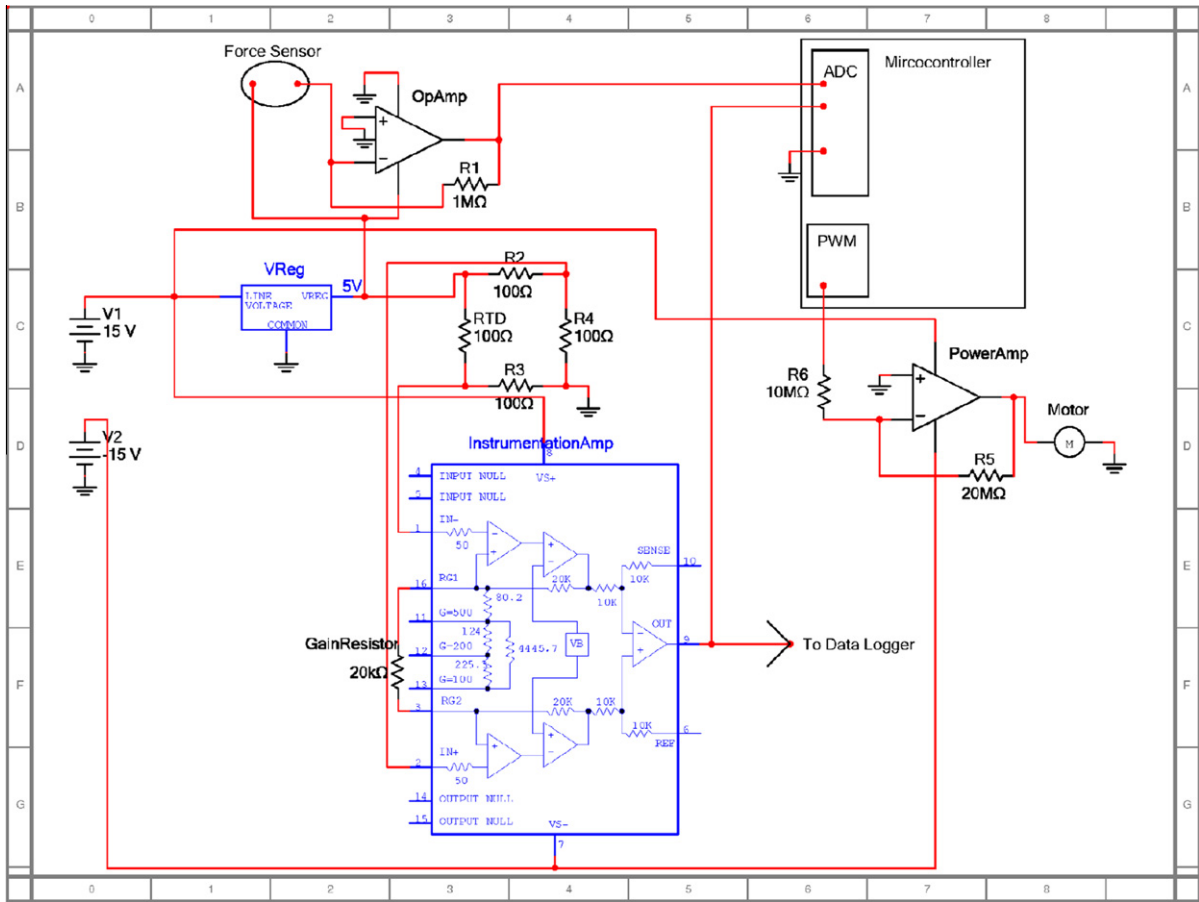


Fig. 2. Circuit diagram of the glove system.

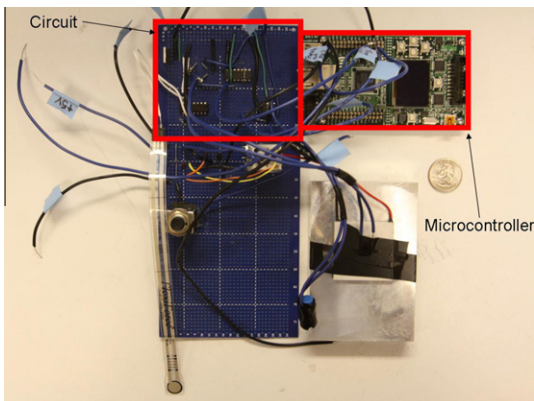


Fig. 3. Photograph of the prototype of the glove system.

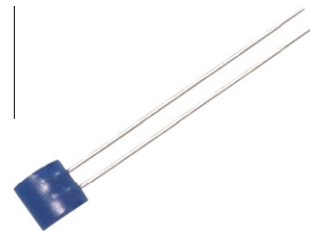


Fig. 4. RTD used in the glove system.

significant range in temperature for most users' purposes. If a larger or different temperature range is needed, similar devices are available to conform to the user's needs. The device has a resistance of 100 Ω at 0 °C, and varies linearly with temperature ( $\alpha = 0.00385 \Omega/\Omega/^\circ\text{C}$ ).

A calibration plot of voltage (V) vs. temperature (C) is shown in Fig. 5. To obtain this plot, the temperature of a

surface exposed to the RTD was increased in steps, and the corresponding voltages were recorded (the voltage corresponds to the voltage sent to the microcontroller). Fig. 5 shows the linear relationship between temperature and voltage output of the RTD. A least-squares fit of the relationship was determined to be:  $V = 0.0131T$ , where  $V$  is voltage (V) and  $T$  is temperature ° (C). The accuracy of the fit was excellent with a value of  $R^2 = 0.988$ .

### 2.3. Force sensor

A Tekscan, FlexiForce piezoresistive force sensor (Model No. A201) was used as an on/off switch in the glove system

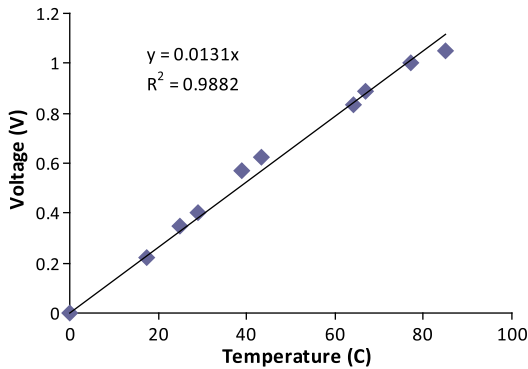


Fig. 5. Calibration of the RTD sensor. The voltage corresponds to the voltage as measured by the microcontroller.

[9]. A photograph of the force sensor is shown in Fig. 6. The sensor is extremely flexible and thin (sheet-like), allowing it to be placed in the glove system without affecting the user's ability to perform tasks. The sensor has a useful range of 0–45 kg with an accuracy of  $\pm 0.45$  kg. The applied force and resistance of the sensor are inversely proportional, with the resistance at zero load equal to 5 M $\Omega$ . No calibration curve was necessary for this device as only one value was needed to serve as the threshold on/off value.

#### 2.4. Micromotor

The final component incorporated into the tactile temperature sensing system was a vibrating micromotor. The purpose of the micromotor was to induce a vibration on the skin of the system's user with a frequency that corresponds to a given temperature. The frequency of this vibration is the varying component that allows a user to distinguish between different temperatures. The temperature and frequency of the micromotor vary linearly, with an increasing temperature corresponding to an increasing frequency of vibration. A photograph of the micromotor used in this system is shown in Fig. 7.

The micromotor shown in Fig. 7 has a diameter of 4 mm and a length of 10 mm. It has a voltage input range of 1–6 VDC, and the rotating unbalanced weight causes the motor to vibrate at a frequency related to the rotational velocity of the motor. The motor was calibrated by measuring its rotational velocity for a given applied voltage. The calibration plot is shown in Fig. 8, and it can be noted that there is a linear relationship between the motor speed (RPM) and the applied voltage (V). The calibration equation is given by:  $MS = 2260.5(V) + 1737.4$ , where  $MS$  is the



Fig. 6. Force sensor used in the glove system.

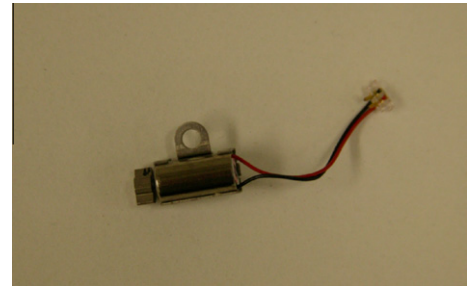


Fig. 7. Micromotor used in the glove system.

motor speed (RPM) and  $V$  is the voltage (V). The least-squares fit is good with a value of  $R^2 = 0.964$ .

### 3. Experimental methods

#### 3.1. Procedure

A testing procedure was developed and a test setup was built in order to examine the ability of the temperature sensing glove to translate the temperature felt by the glove into a tactile sensation. The test setup is shown in Fig. 9. In the test procedure, a stochastic binary input was used to either heat or cool a Peltier device. The temperature sensor on the glove was used to measure the temperature of the Peltier device and the microcontroller on the glove was used to translate this temperature into the vibration frequency of the motor. The user was asked to press a button when they thought the temperature of the Peltier device was increasing based on the vibration frequency they felt from the motor. A baseline test was also performed where the user was also asked to touch the Peltier device directly and repeat the button pushing test. From the data collected, a transfer function of the device was found and response times of the person were determined when using both the motor and his finger. These results are presented in Section 4.

#### 3.2. Experimental design

In the experimental test setup, a data logger was used to record the temperature the RTD sensor measured, the stochastic binary input to the Peltier device, and when

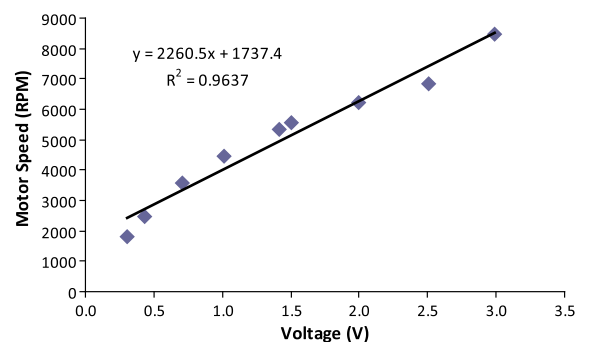


Fig. 8. Calibration of the micromotor.

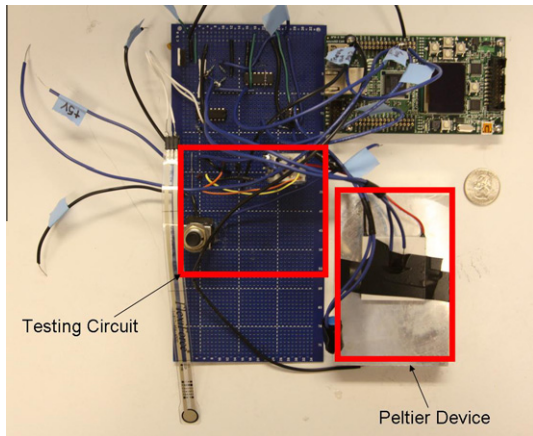


Fig. 9. Photograph of the test device.

The circuit diagram shown in Fig. 11 gives a more detailed description of the testing setup. A digital output channel on the microcontroller was used to send either + 3.3 V or 0 V to a transistor attached to the relay. When the output of the microcontroller was + 3.3 V, the transistor was on and the relay circuit was closed allowing 5 V to be sent through the relay. When 0 V was output from the microcontroller, the transistor was off causing the relay circuit to open and no current to flow through the relay. The relay switches between sending + 5 V or -5 V through the Peltier device depending on whether there is current flowing through the relay. Therefore, the stochastic binary output from the microcontroller was used to control whether the Peltier device was heating or cooling.

A pushbutton switch was also connected to the + 3.3 V pin on the microcontroller. When the button was pushed, the switch was closed and + 3.3 V was sent to the data logger. The data logger was a 10 bit analog-to-digital converter similar to the one on the microcontroller used to read in data from the temperature and force sensors. In addition to recording whether the user was pushing the pushbutton or not, the data logger was also connected to the output of the microcontroller used to run the Peltier device, and to the output of the instrumentation amplifier attached to the RTD. This data was then used to determine the system transfer function and user reaction time to a temperature input.

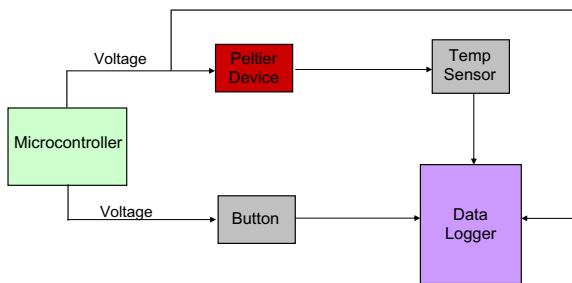


Fig. 10. Block diagram of the test device and data logger.

the user was pressing the button, as shown in the block diagram in Fig. 10.

### 3.3. Power supply

Two different power supplies were used during the experiments. A Kepco multiple output power supply (Model No. MPS 620 M) provided the + 15 V and -15 V needed

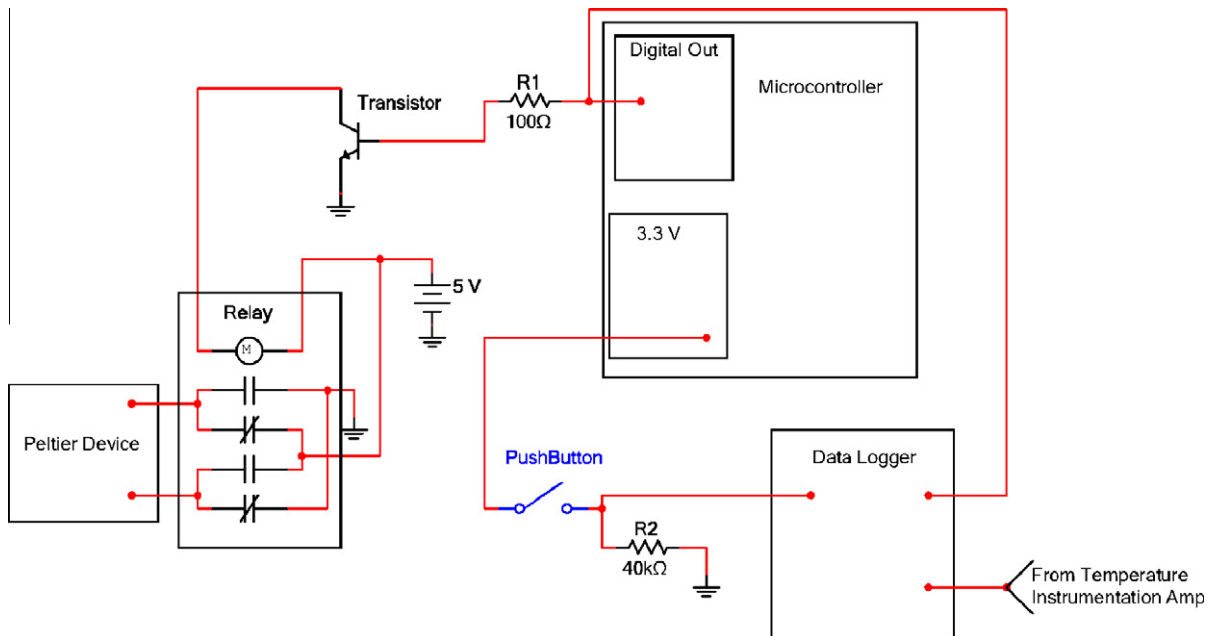


Fig. 11. Circuit diagram of the test device.

to run the glove [10]. An Agilent Technologies triple power output supply (Model No. E3631A) provided the 5 V needed to run the Peltier device [11].

#### 4. Results

It was determined that the best system to identify in terms of discovering a transfer function was the on/off signal sent to the Peltier device as the input and the temperature reading from the RTD as the output. This system was selected because it was the most linear system in the device. The other systems involved a human pressing a push-button. Therefore, it was thought best to analyze the systems that incorporated a human response with the cross-correlation function in order to determine the delays between output and input instead of trying to use a linear system identification technique on an inherently nonlinear system.

##### 4.1. Peltier-temperature system identification

The input sent to the Peltier device consisted of stochastic on and off commands. As seen in Fig. 12, when the value of the input was a one, voltage was connected such that the Peltier device increased in temperature and when the input was a zero, the voltage was reversed which decreased the temperature of the Peltier device. As shown, the input was stochastic in nature. The minimum length of time that the Peltier was in the on or off position was two seconds. After two seconds, the Peltier device was given a new stochastic decision to heat or cool. Fig. 13 is the same data, only it has been detrended so that the mean is zero. This is a necessary precursor to linear system identification.

The output of the RTD is shown in Fig. 14. As seen, the temperature trends upwards over time. This is consistent with the fact that the Peltier device gets warmer simply as a function of time until a steady state temperature is reached. It is important to note that the temperature increases and decreases frequently, which should correspond to the on/off input sent to the Peltier device. Fig. 15 is the same temperature data, only it has been detrended so that the mean is at zero.

The autocorrelation function of the detrended Peltier input is shown in Fig. 16. It is important to note that there is a spike in the autocorrelation function at a lag of 0 s and then the autocorrelation function drops to a value near zero and continues to oscillate around zero for all lags after 0 s. This is consistent with the expected autocorrelation of a stochastic input. The cross-correlation function between the detrended Peltier input and the detrended temperature output is shown in Fig. 17. As seen, there is a spike in the cross-correlation function at a lag of 3 s. This implies that the temperature output of the RTD lags the input of the Peltier device by 3 s.

The experimentally determined impulse response function is shown in Fig. 18. The impulse response was obtained by first taking the Fourier transform of both the autocorrelation and cross-correlation functions, i.e. Figs. 16 and 17, respectively. Then, the Fourier transform of the cross-correlation function was divided by the Fourier transform of the autocorrelation function. Last, the result

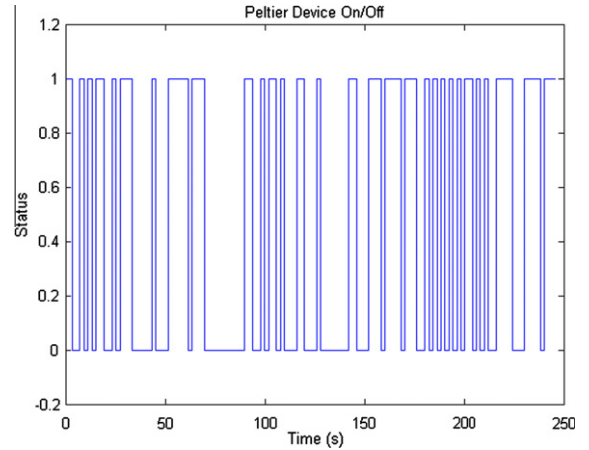


Fig. 12. Stochastic input to the Peltier device.

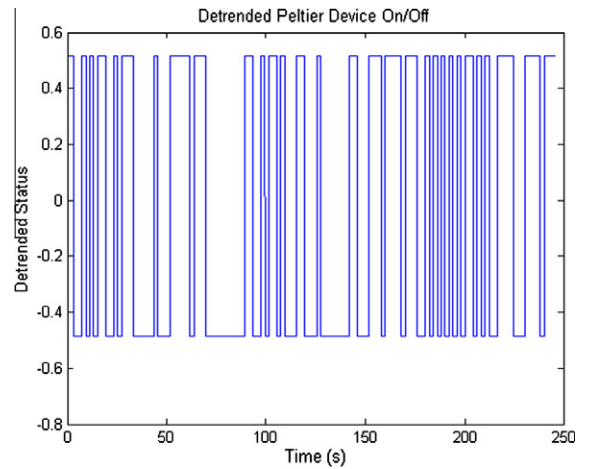


Fig. 13. Stochastic, detrended input to the Peltier device.

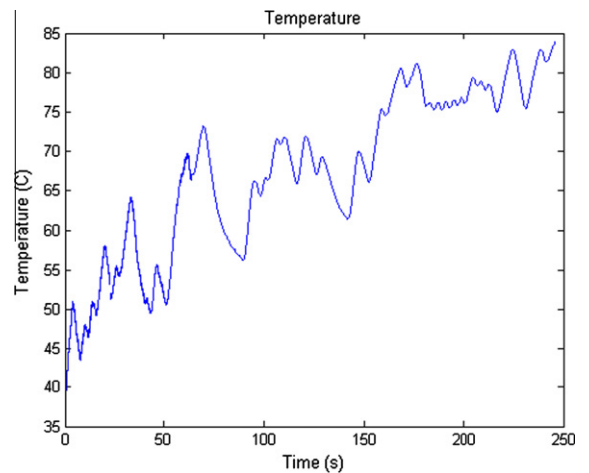


Fig. 14. Temperature output from the RTD as a function of time.

of that division was then transformed back into the time domain by using an inverse Fourier transform. This result is the impulse response function, shown in Fig. 18.

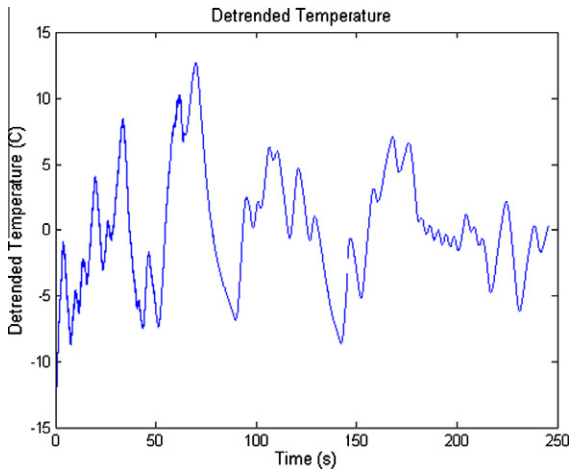


Fig. 15. Detrended temperature output from the RTD.

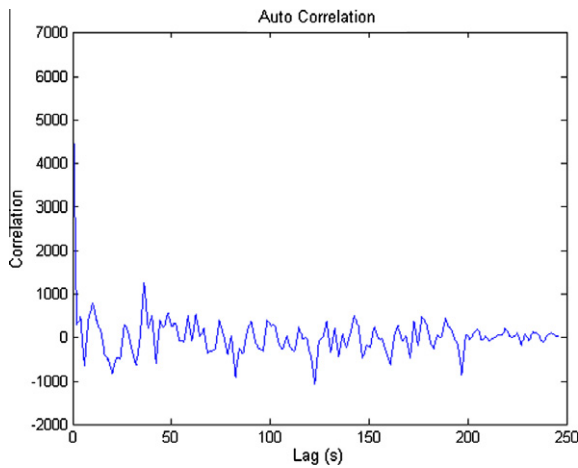


Fig. 16. Autocorrelation function of the detrended, stochastic Peltier input.

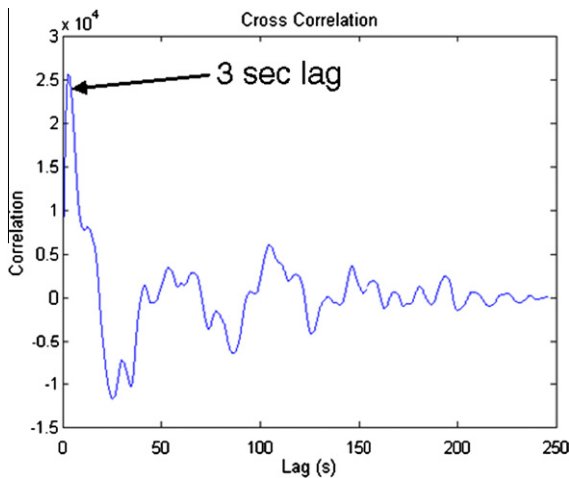


Fig. 17. Cross-correlation function between the detrended, stochastic Peltier input and the detrended, RTD temperature output.

The experimentally determined impulse response function was then fit using the assumption that the system has a first-order response. The experimentally determined impulse response function, shown in red, and the fit of the first-order model impulse response function, shown in blue, are shown in Fig. 19. The transfer function for the Peltier input–RTD temperature output system, assuming a first-order model, is given by:

$$G(s) = \frac{0.2708e^{(-0.3s)}}{5.929s + 1} \tag{1}$$

The experimentally determined impulse response function was also fit using the assumption that the system has a second-order response. The experimentally determined impulse response function, shown in red, and the fit of the second-order model impulse response function, shown in blue, are shown in Fig. 20. The transfer function for the Peltier input–RTD temperature output system, assuming a second-order model is given by:

$$G(s) = \frac{0.3094}{7.398s^2 + 5.562s + 1} \tag{2}$$

4.2. System response with motor

It was determined that the delay due to the human/motor interface should be determined using two different inputs. The first input was the detrended RTD temperature as the input and the response of a human pressing the push-button (when the motor was used to sense temperature) as the output. The second input was the detrended Peltier signal as the input and the response of a human pressing the pushbutton (when the motor was used to sense temperature) as the output.

4.3. Temperature (via motor)-pushbutton delay

Fig. 21 shows the detrended RTD temperature signal. Fig. 22 shows the detrended output of a human pressing a pushbutton. The positive values in Fig. 22 correspond to the human believing that the temperature was increasing via the motor. The negative values correspond to the

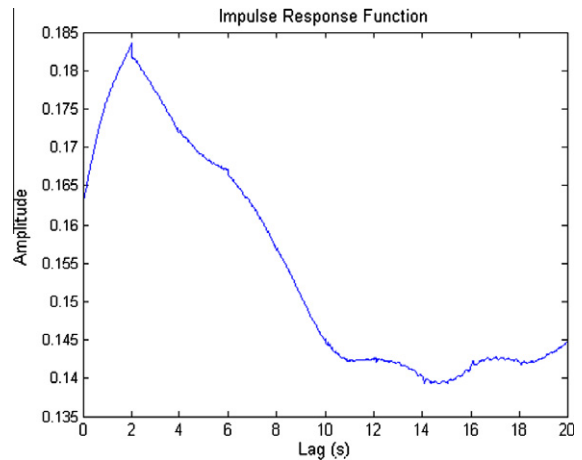


Fig. 18. Impulse response function of the Peltier input–RTD temperature output system.

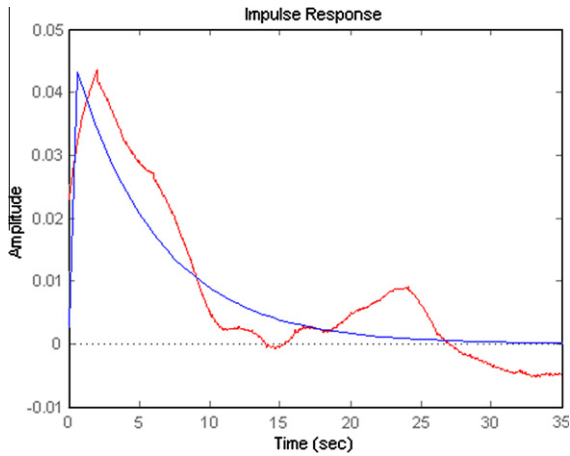


Fig. 19. Experimentally determined impulse response function, red, and the first-order model impulse response function, blue. (For interpretation of the references to colour in this figure legend, the reader is referred to the web version of this article.)

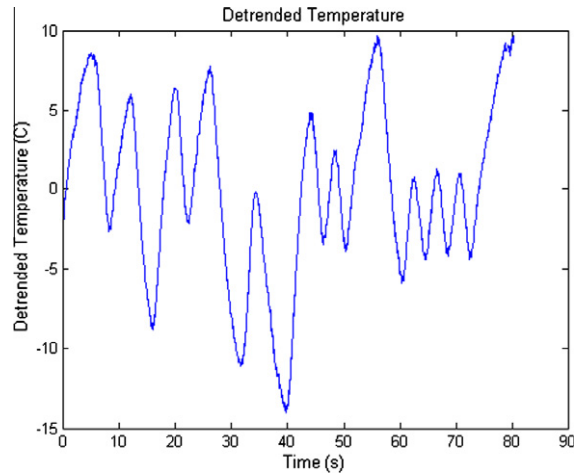


Fig. 21. Detrended temperature from the RTD as a function of time.

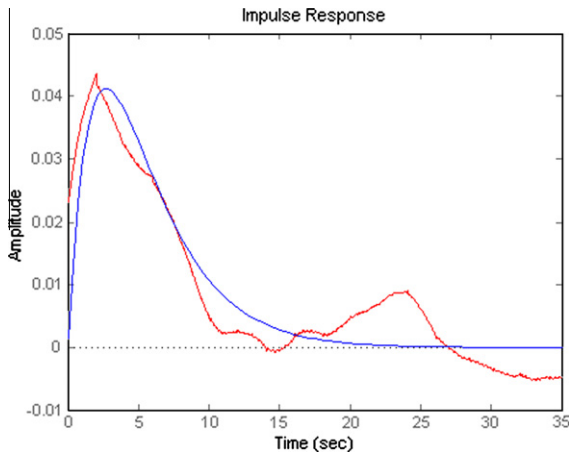


Fig. 20. Experimentally determined impulse response function, red, and the second-order model impulse response function, blue. (For interpretation of the references to colour in this figure legend, the reader is referred to the web version of this article.)

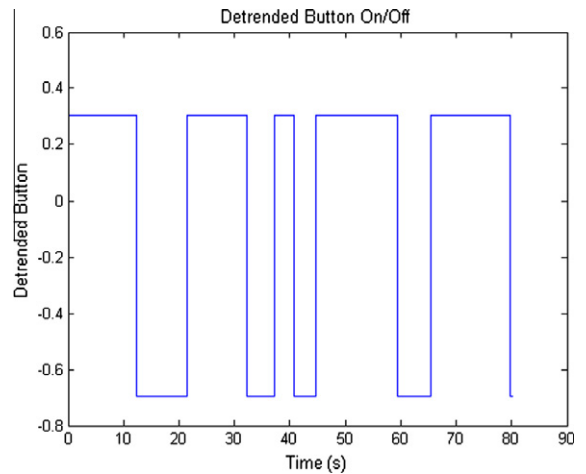


Fig. 22. Detrended output of a human pushing a button.

human believing that the temperature was decreasing via the motor.

Fig. 23 shows the cross-correlation function between the detrended temperature input and the detrended pushbutton output. It is important to note that there is a peak in the cross-correlation at a lag of 4 s. This implies that the delay between the temperature increasing and a human registering that temperature increase via the motor is 4 s.

4.4. Peltier-pushbutton delay

Fig. 24 shows the detrended Peltier device input signal. Fig. 25 shows the detrended output of a human pushing a button. Fig. 26 shows the cross-correlation function between the detrended Peltier device input and the detrended pushbutton output. It is important to note that there is a peak in the cross-correlation at a lag of 6 s. This implies

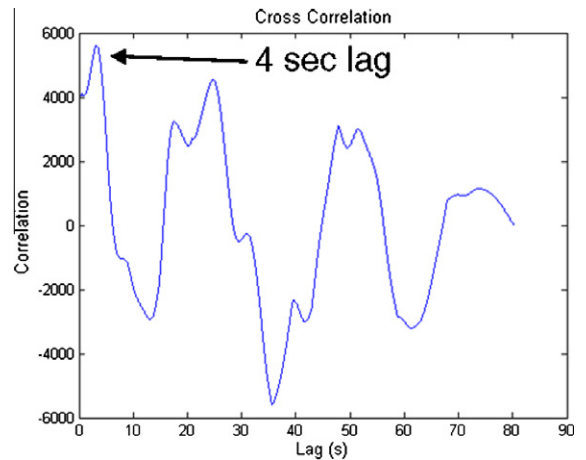


Fig. 23. Cross-correlation function between the detrended, RTD temperature input and the detrended, pushbutton output.



that the delay between the Peltier device being instructed to increase in temperature and a human registering that the temperature increased via the motor is 6 s.

4.5. System response with finger

It was decided that in order to compare the delay due to the human/motor interface, the delay due to a human using his finger should be determined. The human delay using his finger to sense temperature changes, instead of a motor, was determined using two different inputs. The first input was the detrended RTD temperature as the input and the response of a human pressing the pushbutton (when a human’s finger was used to sense temperature) as the output. The second input was the detrended Peltier signal as the input and the response of a human pressing the pushbutton (when a human’s finger was used to sense temperature) as the output.

4.6. Temperature (via finger)-pushbutton delay

Fig. 27 shows the detrended RTD temperature signal. Fig. 28 shows the detrended output of a human pushing a button when using his finger to sense temperature. The positive values in Fig. 28 correspond to the human believing that the temperature was increasing. The negative values correspond to the human believing that the temperature was decreasing.

Fig. 29 shows the cross-correlation function between the detrended temperature input and the detrended pushbutton output. It is important to note that there is a peak in the cross-correlation function at a lag of approximately 0 s. This implies that the delay between the temperature increasing and a human registering that temperature increase via his finger is almost zero.

4.7. Peltier-pushbutton delay

Fig. 30 shows the detrended Peltier device input signal. Fig. 31 shows the detrended output of a human pushing a button when using his finger to sense temperature. Fig. 32 shows the cross-correlation function between the detrend-

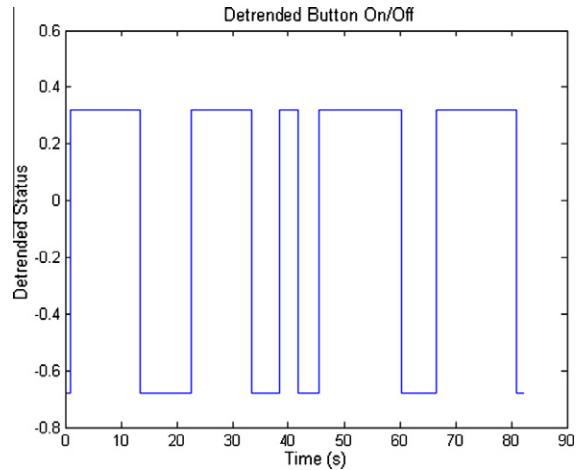


Fig. 25. Detrended output of a human pushing a button.

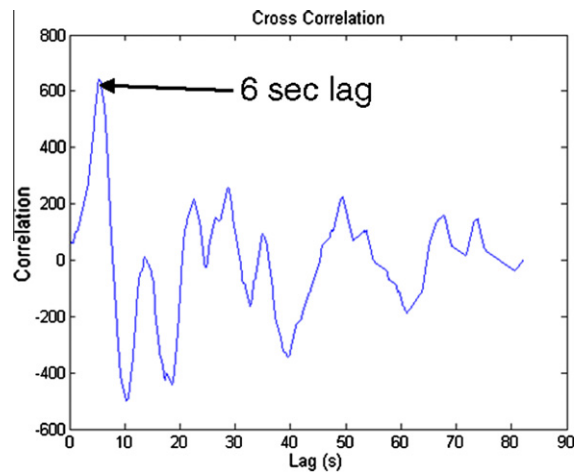


Fig. 26. Cross-correlation function between the detrended, Peltier device input and the detrended, pushbutton output.

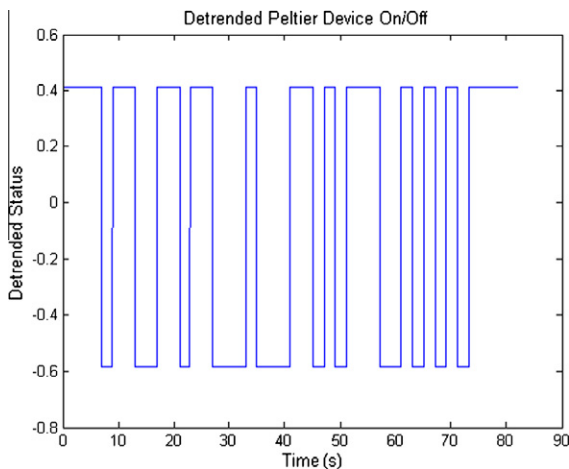


Fig. 24. Detrended Peltier device input as a function of time.

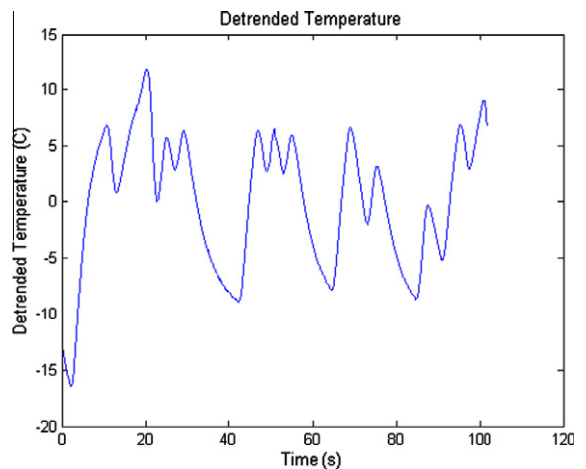


Fig. 27. Detrended temperature from the RTD as a function of time.

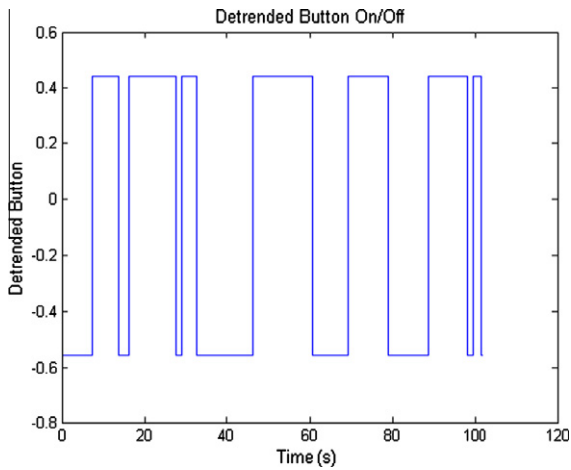


Fig. 28. Detrended output of a human pushing a button.

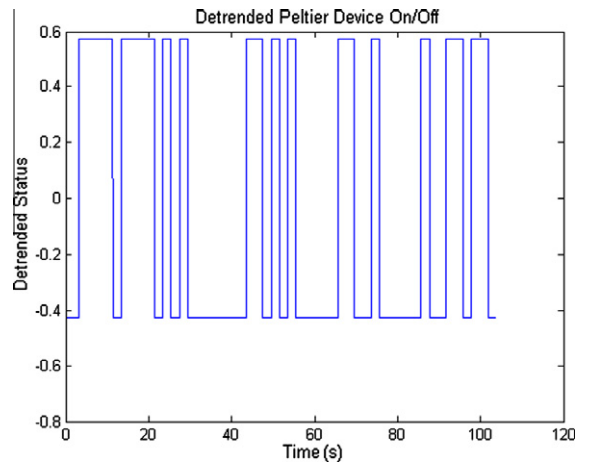


Fig. 30. Detrended Peltier device input as a function of time.

ed Peltier device input and the detrended pushbutton output. It is important to note that there is a peak in the cross-correlation at a lag of 4 s. This implies that the delay between the Peltier device being instructed to increase in temperature and a human registering that the temperature increased via a finger is 4 s.

4.8. Noise analysis

The noise in the temperature signal of the RTD was determined by recording the output of the RTD in the absence of a temperature change. Fig. 33 shows the temperature signal that was recorded when there was no temperature change taking place. As can be seen, there is noise in the data. The average value of temperature that was recorded was 42.1 °C and the standard deviation of the signal was 0.85 °C. Fig. 34 shows a histogram of the amplitude of the noise signal. As shown in Fig. 34, the noise does appear to be Gaussian.

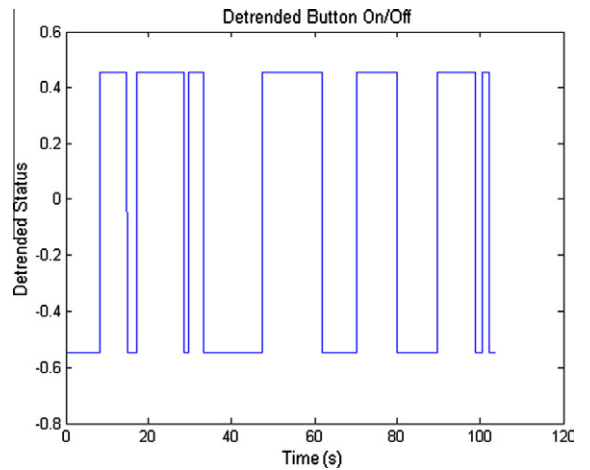


Fig. 31. Detrended output of a human pushing a button.

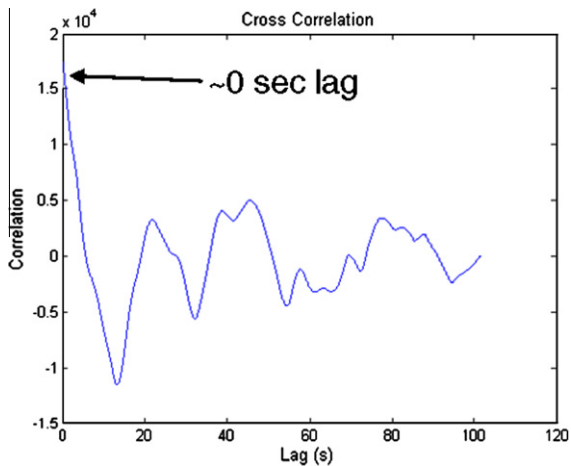


Fig. 29. Cross-correlation function between the detrended, RTD temperature input and the detrended, pushbutton output.

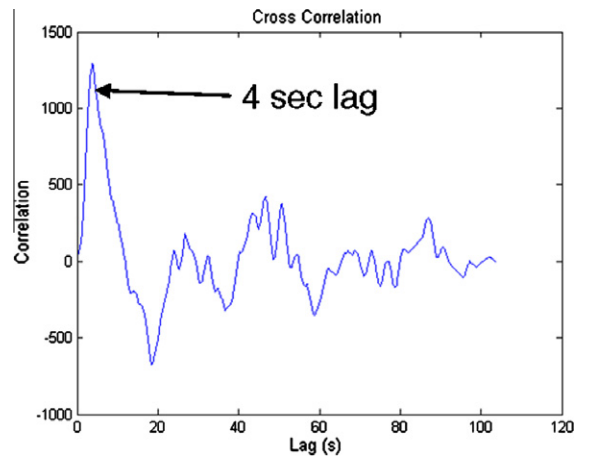


Fig. 32. Cross-correlation function between the detrended, Peltier device input and the detrended, pushbutton output.

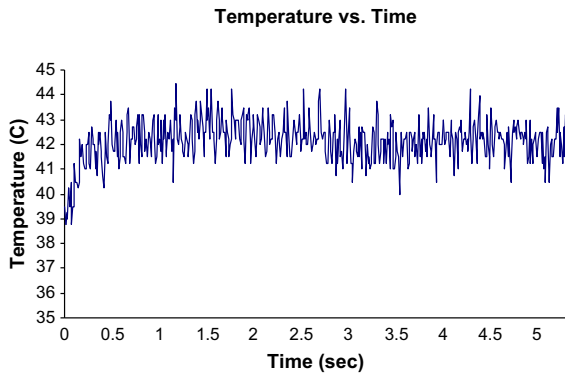


Fig. 33. Temperature output of the RTD when no temperature change is taking place.

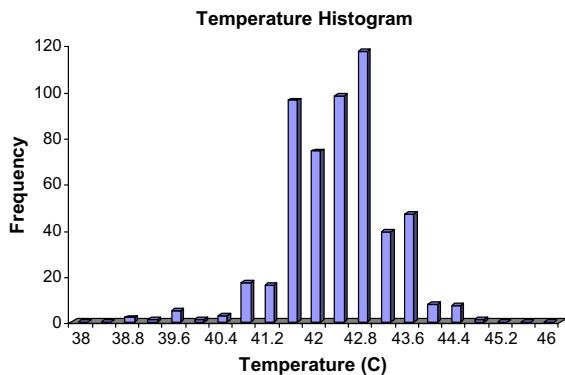


Fig. 34. Histogram of the amplitude of the temperature output of the RTD when no temperature change is taking place.

## 5. Conclusions

A glove was developed that converts temperature into a vibrating frequency that can be felt by the user. Linear system identification analysis was performed to determine the transfer function between the Peltier device on/off signal as the input and the temperature measured by the RTD as the output. Both first-order and second-order transfer functions were successfully determined for the system. Although it was believed that the temperature response of the glove would best be described by the first-order transfer function, it was evident that there were other system dynamics in the glove's electronics. Therefore, it was determined that the second-order transfer function was the best fit for the Peltier input-temperature output system. It was also determined that there is a 3 s delay

between the Peltier device being instructed to increase in temperature and when the increase in temperature is measured by the glove.

It was also determined that there is a 4 s delay between the temperature of an object increasing and a human detecting that temperature increase when using the micro-motor in the glove. In addition, it was determined that there is almost no delay (i.e.  $\sim 0$  s delay) between the temperature of an object increasing and a human detecting that temperature increase when using his finger. This result was expected. The benefit of the glove system is that it can be used to sense temperatures that an unprotected human finger would otherwise not be able to withstand.

The noise in the temperature reading of the glove system was determined to be Gaussian and had a standard deviation of 0.85 °C.

## Acknowledgements

The authors would like to thank Mr. Adam Wahab for all of his help, time, support, and patience. Without him, this research would not have been possible. Thanks are also due to Prof. Ian Hunter for many helpful suggestions and to Mr. Scott McEuen for helping with the microcontroller.

## References

- [1] P. Bach-y Rita, C.C. Collins, F. Saunders, B. White, L. Scadden, Vision substitution by tactile image projection, *Nature* 221 (1969) 963–964.
- [2] P. Bach-y-Rita, S.W. Kercel, Sensory substitution and the human-machine interface, *Trends Cogn. Sci.* 7 (12) (2003) 541–546.
- [3] P. Bach-y-Rita, J.G. Webster, W.J. Tompkins, T. Crabb, Sensory Substitution for Space Gloves and Space Robots, Space Telerobotics Workshop, Jet Propulsion Laboratory, Pasadena, CA, January 1987, pp. 51–57.
- [4] H.J. Boll, Sensory substitution system, US Patent 3766,311, 1973.
- [5] G.D. Havey, P.L. Gibson, G.J. Seifert, S. Kalpin, Method and apparatus for sensory substitution, vision prosthesis, or low-vision enhancement utilizing thermal sensing, US Patent 7308,314 B2, December 2007.
- [6] D.G. Caldwell, C. Gosney, Enhanced Tactile Feedback (Tele-Taction) using a Multi-Functional Sensory System, in: IEEE International Conference on Robotics and Automation (1993) 955–960.
- [7] Luminary Micro, Stellaris Microcontroller, Model No. LM3S8962, <[http://www.omega.com/ppt/pptsc.asp?ref=F1500\\_F2000\\_F4000&Nav=temc13](http://www.omega.com/ppt/pptsc.asp?ref=F1500_F2000_F4000&Nav=temc13)>.
- [8] Omega, OmegaFilm, Flat Profile, Thin Film Platinum RTD, Model No. F2020-100-B-100, <[http://www.omega.com/ppt/pptsc.asp?ref=F1500\\_F2000\\_F4000&Nav=temc13](http://www.omega.com/ppt/pptsc.asp?ref=F1500_F2000_F4000&Nav=temc13)>.
- [9] Tekscan, FlexiForce Piezoresistive Force Sensor, Model No. A201, <<http://www.tekscan.com/flexiforce/specs-flexiforce.html>>.
- [10] Kepco, Multiple Output Power Supply, Model No. MPS 620M, <<http://www.kepcopower.com/mpsbuy.htm>>.
- [11] Agilent Technologies, Triple Output Power Supply, Model No. E3631A, <<http://www.home.agilent.com/agilent/product.jsp?pn=e3631a>>.